A Geostatistical Approach for the Geomatics Characterization of a Landslide Phenomenon

Alberico Sonnessa, Noemi Pagano(✉), and Eufemia Tarantino

Department of Civil, Environmental, Land, Construction, and Chemistry (DICATECh), Politecnico di Bari, Via Orabona 4, 70125 Bari, Italy
{alberico.sonnessa,eufemia.tarantino}@poliba.it,
n.pagano@phd.poliba.it

Abstract. Monitoring ground deformation in urbanized areas is a significant challenge for hydrogeological risk management and land-use planning. Starting from the combination and integration of remote sensing techniques with geostatistical modelling, this study focuses on characterizing, from a geomatic side, an ongoing landslide phenomenon in the municipality of Chieuti (FG), in southern Italy.

The analysis is based on the use of the MT-InSAR (Multi-Temporal Interferometric Synthetic Aperture Radar) technique, applied to data acquired from the Sentinel-1 (S1) constellation. Considering the discrete nature of these measurements, limited to Persistent Scatterers (PS), a geostatistical approach is proposed for the continuous reconstruction of the deformation field.

In particular, the spatial correlation structure was analyzed using an empirical variogram and theoretical modelling. Subsequently, ordinary kriging interpolation was applied to obtain velocity estimates even in areas lacking direct observations, enabling the generation of continuous deformation maps within a GIS environment. The kinematic analysis allowed the identification and delineation of an area of active instability characterized by predominantly vertical deformations. The results showed a high level of consistency, confirming the reliability of the proposed methodology. The integrated approach developed is a useful tool for supporting decision-making in geomorphological risk management, particularly in urban contexts characterized by soil instability phenomena.

Keywords: Geostatistical analysis · SAR · geomatics monitoring · landslides · Kriging

1 Introduction

The interaction between natural evolutionary dynamics of natural phenomena and human pressure—which increasingly gives rise to catastrophic and devastating scenarios—is today one of the most complex challenges facing society and the scientific community. Hydrogeological instability represents one of the most critical and immediate manifestations of this, where the geomorphological fragility inherent to the Earth's surface intersects with the transformative impact of human activity. Given the Italian territory's structural vulnerability and natural predisposition to phenomena such as landslides and

© The Author(s), under exclusive license to Springer Nature Switzerland AG 2027
O. Gervasi et al. (Eds.): ICCSA 2026 Workshops, LNCS 16762, pp. 77–92, 2027.
https://doi.org/10.1007/978-3-032-30524-4_6

subsidence, the impact of the climate crisis and the partially unsustainable management of the territory have exacerbated their magnitude and frequency, expanding their scale. The country's history confirms the urgency of a decisive shift in approach: emergency management of events can no longer substitute for, nor take the place of, a phase of failed or insufficient prevention [1]. The scale of the phenomenon is reflected in the Inventory of Landslide Phenomena in Italy (IFFI Project), compiled by ISPRA, which records over 636000 landslides, covering approximately 8.3% of the national territory. This is a consistent body of data that highlights the intrinsic danger of the peninsula, where approximately 28% of the phenomena are rapid-moving (collapses, mudflows, and debris flows) and highly destructive [2].

The history of this territory has been deeply shaped by its susceptibility to natural disasters, as evidenced by the enduring scars of the Sarno and Quindici disaster (May 1998), the tragic occurrences on the Island of Ischia (November 2022), and the recent landslides that affected the municipality of Niscemi (January 2026) and the Petacciato area in the Molise region (April 2026). These critical occurrences confirm that uncontrolled urbanization and inadequate maintenance act as risk multipliers, with devastating social and economic consequences [3].

A further warning comes from the data in the 2024 ISPRA Report, which estimates that 94.5% of Italian municipalities are currently exposed to risks arising from landslides, floods, or coastal erosion. In this scenario, the resilience of territories becomes directly dependent on the monitoring plans put in place. Tools such as the national IdroGEO platform have now become invaluable instruments for prediction, management, and proper communication of hydrogeological risk [4]. This vulnerability is particularly evident in the Apulian territory, where the necessity of enhancing the resilience of both urban fabric and cultural heritage against extreme weather events has been extensively documented [5–8].

Effective measures to counter deformation phenomena must be based on their proper characterization; one of the tools capable of supporting these objectives is the geomatics-based monitoring. In this case, the development of the European Copernicus program, specifically through S1, has made extensive radar data archives with high spatial and temporal resolution available [9, 10].

The MT-InSAR technique now allows for the detection of millimeter-scale displacements over large areas, providing a fundamental database for both real-time monitoring and retrospective analyses (back-analyses)[11–13].

The temporal and spatial advantages are offset by the inherent disadvantage of the data, namely that it is point-based and discrete.

Displacement information is, in fact, dependent on the presence of stable reflectors (PS), leaving large portions of the territory without direct measurements. This results in a purely deterministic approach that may sometimes be insufficient to describe the complexity of the case, given the uncertainty factors governing it and the fragmented nature of the information.

The transition from a discrete to a continuous nature can be achieved through a probabilistic approach, and geostatistics steps in to bridge this gap [14–17], allowing for the analysis of the spatial correlation structure of the data to transform point-based information into continuous surfaces through estimation techniques such as kriging. It

is thus possible to spatialize the deformation field, quantifying the associated uncertainty and providing a coherent overview even where satellite sensors do not return a signal [18]. The study proposes the application of this methodology to a municipality of Chieuti, located in the Dauno Sub-Apennines area, suffering from an active landslide phenomenon that is still ongoing (Fig. 1). The integration of MT-InSAR data and geostatistical tools aims to reconstruct the spatiotemporal evolution of the landslide accurately, providing decision-making support crucial for the protection of public safety.



Fig. 1. Geographical localization of the study area: the satellite image shows the town center of Chieuti (Apulia Region, southern Italy) and its rural surrounding area (source: Google Maps). The inset map in the upper right corner illustrates the precise geographical location of the study area within the Italian peninsula.

2 The Study Area

The municipality of Chieuti is located in the northern sector of the Apulian territory, on the border between the Apulia and Molise regions. The site is affected by an extensive landslide phenomenon that has historically required continuous interventions by competent authorities to plan appropriate consolidation works. The instability of the slope has been documented since the late 19th century. To mitigate the effects of the movement, various structures have been built since 1950, with the most recent being a retaining wall constructed in 2006 along the critical sector of the slope. Despite these interventions, the continuing subsidence has compromised the structural integrity of several buildings,

making it necessary to declare them uninhabitable. The landslide phenomenon affects both the residential area and the Crojo spring area, which is characterized by complex hydrogeological dynamics and is located northwest of the historic center. The severity of the situation in the area is amply confirmed by official data from the national IdroGEO platform (ISPRA), based on the mosaic of basin-level hydrogeological plans (PAI) (Fig. 2). The risk of landslides affects a significant portion of the local socio-economic fabric: 1.213 km^2 of the territory are classified as High (P3) and Very High (P4) risk, directly affecting 17 buildings and approximately 5.4% of the resident population.

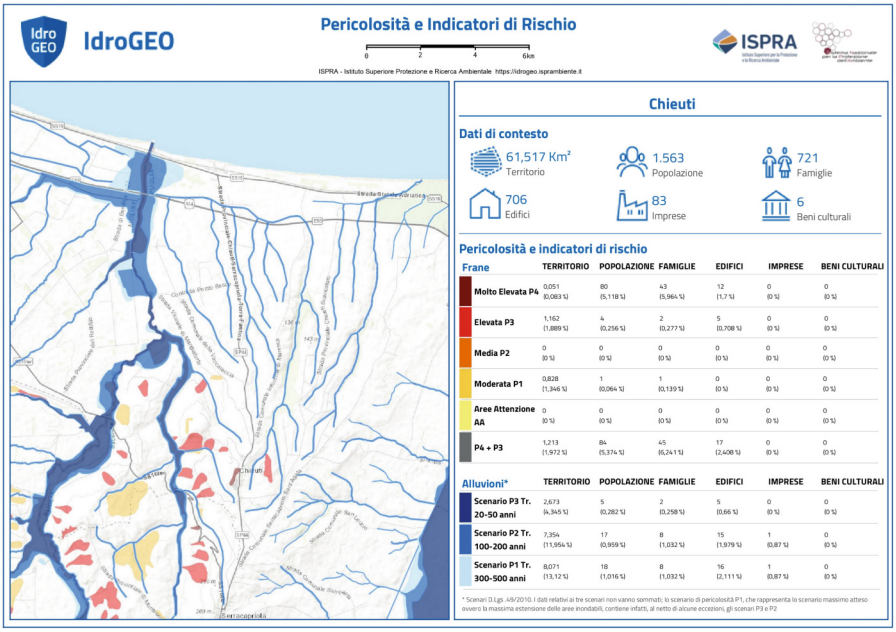

Fig. 2. Landslide and hydraulic hazard indicators for the municipality of Chieuti, according to the national IdroGEO platform (ISPRA).

3 Methodologies Employed

Integrating a geostatistical approach into the analysis workflow was necessary to overcome the intrinsic limitation of the point-based and discrete nature of InSAR data, enabling the transition from a set of scattered measurements to a continuous reconstruction of the deformation field [15]. Assuming the displacement velocity V_LOS as a regionalized variable, the analysis was divided into an exploratory data analysis phase and a subsequent stochastic modeling of spatial dependence.

3.1 The MT-InSAR Technique

The MT-InSAR technique, with its millimeter-level precision in monitoring slow ground displacement velocities over years, is considered a trusted and consistent choice for analyzing ground subsidence in urban contexts.

This methodology takes advantage of the phase difference between radar signals acquired by the SAR sensor at successive times, allowing for the quantification of displacement along the satellite line of sight (LoS). The historical and temporal reconstruction relied on the systematic use of the S1 constellation dataset. By leveraging the high temporal resolution and consistent revisit time of this mission, it was possible to delineate a continuous and coherent deformation history. The S1 Mission of the Copernicus program provided a high degree of temporal continuity thanks to a data archive available since 2015. Despite the moderate spatial resolution (20x5m), the revisit frequency—initially 6 days and 12 days for a limited time interval—ensures the statistical robustness necessary for estimating long-term deformation trends. The technical specifications are further detailed in the table below (Table 1) [8].

Table 1. S1 Mission specifications

Satellite	Acquisition mode	Spatial resolution (Azimuth × Range)	Wavelength (λ)	Orbit	Temporal resolution	Monitoring period	N. of images	Angle of incidence
S1	Interferometric wide-swath	20 m ×5 m	5.6 cm	Ascending	6 days (12 days after Dec. 2021)	Apr 2015-May 2022	367	42.1°
				Descending		Apr 2015-May 2022	361	41.2°

3.2 Geostatistical Analysis

The study of spatial correlation is typically performed through variogram analysis, as it serves as a spatial dependence model that describes data variance between two locations as a function of their distance. The variogram estimates the average degree of variance between values based on their separation in geographic space, defined as

$$\gamma(h)=\frac{1}{2N(h)}\Sigma_{i=1}^{N}\,[Z(u+h)-Z(u)]^2$$

- Z(u) represents the value measured at point (u);
- h is the distance between two points;
- N(h) indicates the number of pairs of points separated by distance (h).

The variogram is, by definition, zero at the origin ($\gamma(0) = 0$), however, as $h \to 0$, it often does not tend to zero, instead tending to a positive definite value. Although the variogram appears to have a non-zero value at the origin, it increases sharply as soon as it moves away from it. This discontinuity can be due to either a sampling grid that is too sparse to capture the microvariability of the natural phenomenon or to measurement errors and is defined as the nugget effect. If the semivariogram reaches a limit value, allowing the identification of a threshold, there exists a distance known as the range, beyond which the random variables Z(u) and Z(u + h) are no longer correlated. From this

perspective, the range provides a precise definition of the traditional concept of a zone of influence: a variable Z(u) will be correlated with any other variable whose position falls within a neighbourhood centred at (u) with a radius equal to the range. Both the range and the threshold typically depend on the direction along which the semivariogram is defined.

3.2.1 Ordinary Kriging

To switch from a point-based representation to a continuous, deformable surface, the Ordinary Kriging (OK) technique was applied. This stochastic interpolation method allows for the estimation of the displacement velocity at unsampled points in the domain, minimizing the variance of the error.

The estimation of kinematic variables at unsampled points is central to determining the displacement field, allowing the transition from a point-based representation to a continuous surface. To obtain an estimate of the variables under investigation at unsampled points, a stochastic interpolation technique called Kriging is used. The technique employs information derived from observed values at certain points in the domain and allows for the evaluation of the dynamics of the characteristic of interest at points within the same domain with no available data. Accuracy depends on several factors, such as the number of observations and data quality, the geometry of the sampled points, the distance between points, and the uniformity of the spatial variable under examination. Kriging is an estimation method that allows for the appropriate consideration of all the factors listed above. In particular, the term "kriging" is used in spatial statistics as a synonym for "optimal estimation method," as it is capable of making the best use of observations from points near the point of interest.

In general, for each unsampled point u_o where the value of the variable $Z(u_o)$ is unknown, the estimate $Z^*(u_o)$ is determined using a weighted linear combination of a set of sampled values $Z(u_i)$ within the same domain of interest:

$$Z^*(u_o) = \Sigma_{i=1}^{N} \lambda_i Z_{(u_i)}$$

where λ_i represents the Kriging weights assigned to each observed point $Z(u_i)$.

Prediction maps are subsequently generated by calculating the estimated value $Z^*(u_o)$ for each cell of a regular grid covering the study area.

3.3 Cross-Validation

A cross-validation technique has been applied to compare the expected values with the observed values using only sample data. This procedure enables the comparison of different models and the selection of the one that best fits the kinematics of the object of study.

Operationally, the cross-validation method encompasses dividing the PS database into multiple subsets; in turn, the values at specific points are temporarily removed from the set of available observations to be subsequently estimated using the remaining data and the variogram model under test. It is essential to note that the points subject to validation are not used in any way in the geometry used to estimate them, thus ensuring the impartiality of the statistical test.

Once the procedure is completed for all sub-databases, the observed values are compared with the predicted values by calculating the multiple coefficients of determination R^2 and analysing the slope of the regression line.

4 Results and Discussion

4.1 Dataset Selection and Domain Definition

The geostatistical analysis phase was preceded by a rigorous process of selecting and preprocessing the SAR data. The estimated variables are the average annual displacement velocity (mm/year) and the overall displacement (mm), both measured along the LoS. Negative values indicate that the distance between the satellite sensor and the PS is increasing, meaning the sensor is moving away from the PS, which is consistent with the slope kinematics. For the Chieuti case study, a S1 dataset collected in the descending orbit was used. The S1 MT-InSAR dataset employed in this study was not processed ex novo for the current research. Rather, this work builds upon a previously validated product. The entire interferometric processing chain, including the data extraction stages and validation procedures, has been extensively documented in previous studies [12, 20].

Figure 3 shows the spatial distribution of average velocities in the historic center: the color scale highlights the most critical sectors in red (velocities between -12 and -10 mm/year) and stable areas in blue (0 to + 2 mm/year).

To ensure the robustness of the deformation field, the quality of the PSs was assessed using the coherence parameter (COH), which ranges from 0 to 1. Specifically, within the study area, the S1 dataset consists of 1,713 sampled points, of which approximately 80% (1,394 PS) have a COH value greater than 0.5, while 30% of the dataset (544 points) maintain a COH greater than 0.8. By using the high-coherence PS, considered trustworthy for describing the landslide's temporal evolution, there is an attempt to minimize uncertainty during the subsequent geostatistical interpolation phase.

The application of ordinary kriging could only be continued once the trend had been analysed and the variogram had been examined. The variogram has reached a plateau (Sill), which means that the mean is locally stationary. This confirms that Kriging is the appropriate method and that there is no need to complicate the model with deterministic polynomials.

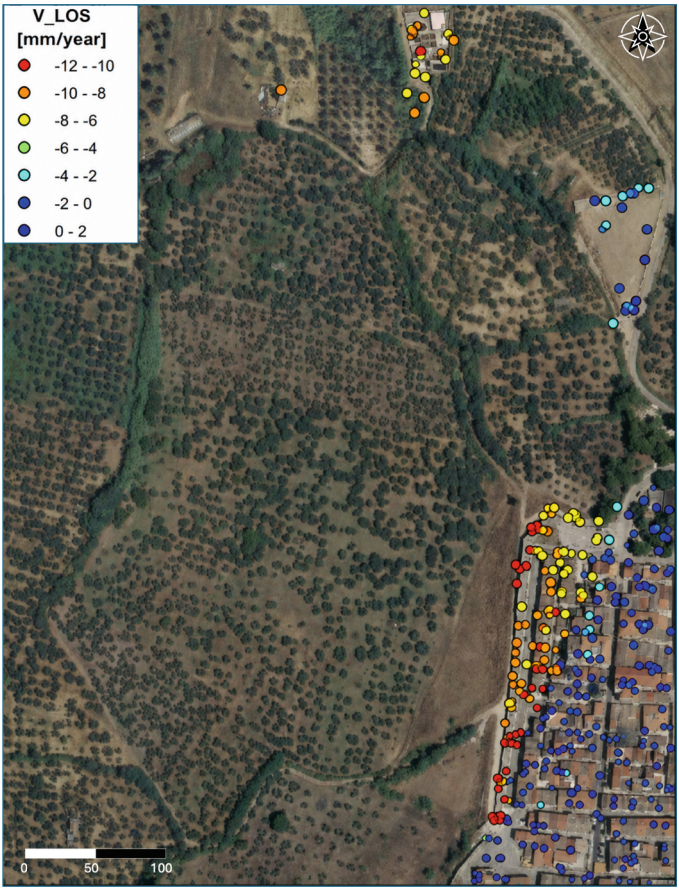

Fig. 3. Spatial distribution of average annual displacement velocities (V_LOS) in the historic center of Chieuti

4.2 Analysis of Entropy and Anisotropy

However, to better characterize the system's stability and study local variations, Voronoi entropy analysis was incorporated into the study. The method is based on dividing the study area into polygons, where each cell is defined such that any point within it is geometrically closer to its own "generating point" than to any other PP present in the dataset [21].

Through this spatial subdivision, it was possible to calculate the local entropy, a parameter that measures the degree of disorder or distortion in the velocity field. An entropy close to zero indicates homogeneous kinematic behaviour (stability or block motion), while high values signal strong heterogeneity among the displacement vectors of adjacent PSs (Fig. 4). This analysis allows to link the the magnitude of the displacement with the presence of differential settlements. Likewise, variability—particularly in terms of spatial and directional velocity—was identified through semivariogram analysis, which revealed marked anisotropy in the system. These statistics have a direct

interpretation in the territory and an objective correlation in the area under study, as the spatial distribution of pairs of points with maximum variance at short distances accurately reflects the geometry of the cracks and structural settlements detected in the buildings on the western slope.

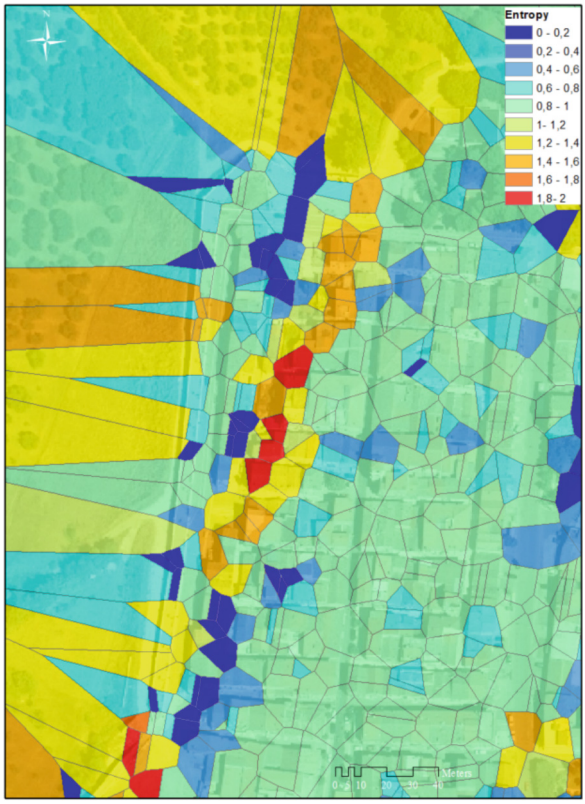

Fig. 4. Local entropy map derived from Voronoi tessellation of the PS dataset.

The presence of pairs of PSs with significantly contrasting velocity values just a few meters from each other—located along the western slope, where the maximum velocity gradients are recorded—cannot be interpreted as a simple measurement error, nor can it be mistaken for an isolated data anomaly. Instead, it constitutes the kinematic manifestation of a discontinuity in the ground; where the diagram shows a marked jump in variance, the physical reality reveals a fracture line that causes damage and differential settlements in the structures.

4.3 Modelling and Validation of the Semivariogram

After the exploratory analysis, it was decided that the theoretical model that best matches the spatial correlation structure of V_LOS is the spherical model. This is described by

a threshold (sill) of 6.2 $(mm/year)^2$, a value that indicates the reach of local stationarity of the variance. The key to the modelling is the integration of geometric anisotropy. As previously discussed, statistical weights do not get assigned in an isotropic method (equal in all directions) in Ordinary Kriging, but rather follow the kinematic morphology of the slope, which is characterised by two directions: that of maximum continuity and that of maximum variance. The direction of maximum continuity—the orientation along which the ground exhibits the most homogeneous behaviour, enabling the model to 'trust' nearby points more for estimation and assigning the highest weights—is equal to 20°.

The anisotropy of the model is defined by the polar angle α of the orientation of the search ellipse and its major and minor semi-axes. Setting a maximum search radius of 90 m enables micro-variations in the annual average velocity to be accurately mapped, ensuring the local kinematic trend is preserved.

Model validation is based on the procedure described above; therefore, the dataset consisting of S1 pixels segregated by coherence (greater than 0.5) and identified within the study area (Fig. 5) has been divided into two equal parts identified by the codes S1_COH05_01 and S1_COH05_02, whose characteristics are shown in the following table (Table 2).

Table 2. Characteristics of the validation and training subsets (S1_COH05_01 and S1_COH05_02) split for cross-validation

Dataset	Satellite	Acquisition Mode	Spatial resolution	Revisit time	Orbit	N. of Images	Number of PS
S1_COH05_01	Sentinel-1	IW-Swath	20x5m	16 days	Descending	361	**719**
S1_COH05_02	Sentinel-1	IW-Swath	20x5m	16 days	Descending	361	**719**

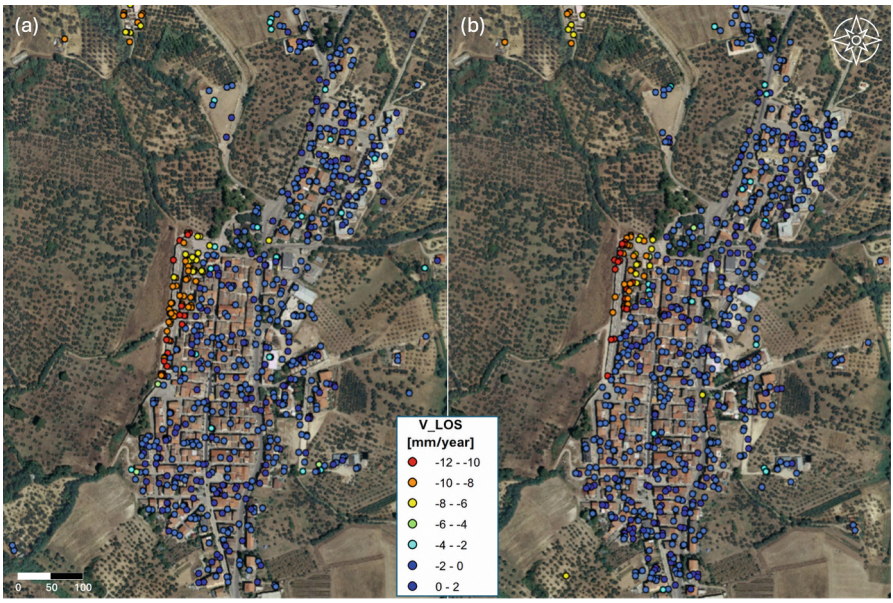

Fig. 5. Validation (a) and training subset (b) (S1_COH05_01 and S1_COH05_02) spatially displayed within the study area for cross-validation purposes

Following the validation phase, the optimized geostatistical parameters (spherical model, 20°/110° anisotropy, and 90-m search radius) were applied to generate the continuous surface of the deformation velocity V_LOS across the entire investigation area. The subsequent stage entailed the creation of a prediction map employing ordinary kriging with one of the two datasets, utilising the second dataset as the validator and advancing to the cross-validation phase.

This process was then repeated with the two datasets swapped.

The multiple R^2 coefficient obtained was 0.85 and the slope of the regression line was 0.97. The variogram model was chosen as it showed the highest multiple R^2 coefficient value compared to the various repeated models, thus representing the spatial correlation model of V_LOS for the analysed system best. The table below (Table 3) provides a comprehensive overview of the various attempts made.

Table 3. Geostatistical parameters and cross-validation results for the different semivariogram models tested

Input Dataset	Validation Dataset	Angle α [°]	a max [m]	a min [m]	Model	R^2	Slope
S1_COH05_01	S1_COH05_02	20	90	40	Stable	0,77	0,97
S1_COH05_01	S1_COH05_02	20	90	40	Spherical	0,85	0,97
S1_COH05_01	S1_COH05_02	20	90	40	Exponential	0,8	0,97
S1_COH05_02	S1_COH05_01	20	90	40	Stable	0,77	0,95

(*continued*)

Table 3. (*continued*)

Input Dataset	Validation Dataset	Angle α [°]	a max [m]	a min [m]	Model	R^2	Slope
S1_COH05_02	S1_COH05_01	20	90	40	Spherical	0,85	0,97
S1_COH05_02	S1_COH05_01	20	90	40	Exponential	0,8	0,97

Although the S1 dataset is characterized by moderate spatial resolution (20 × 5m) and intrinsic signal noise, the ordinary kriging technique allowed for the effective estimation of kinematic trends. To demonstrate the filtering capability of the optimized spatial model, prediction maps were generated under two different conditions. The final prediction maps are presented below: the first obtained using the complete S1 dataset without consistency-based segregation (Fig. 6) and the second by applying the consistency filter > 0.5 (Fig. 7).

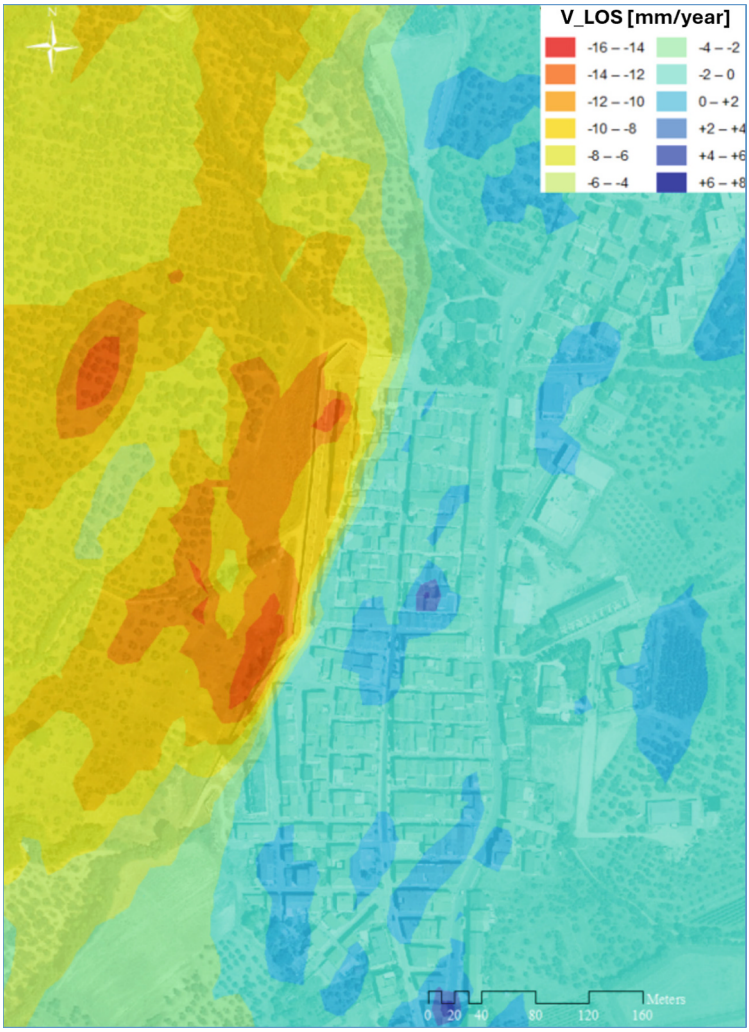

Fig. 6. Continuous V_LOS prediction maps generated via Ordinary Kriging, obtained from the complete S1 dataset without consistency-based segregation

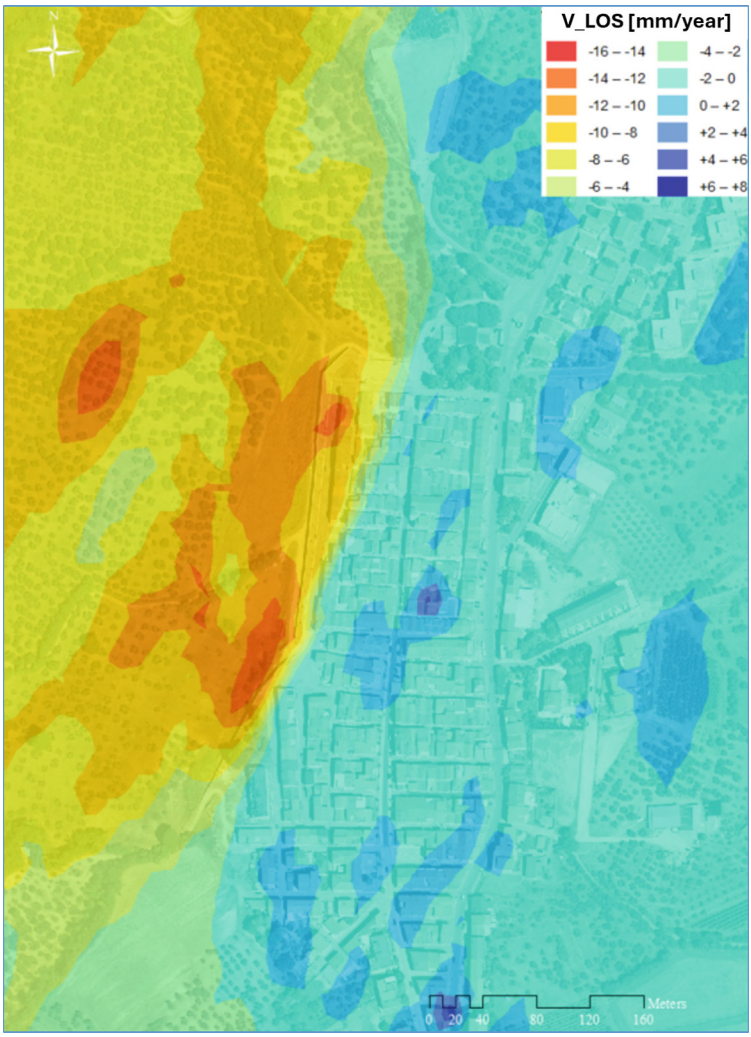

Fig. 7. Continuous V_LOS prediction maps generated via Ordinary Kriging. Obtained from the S1 dataset by applying a coherence filter (COH > 0.5)

5 Conclusions

The present study was developed to delineate a kinematic and spatiotemporal framework of the landslide phenomenon affecting the municipality of Chieuti, by applying a geostatistical approach to geomatic datasets. Although the area has been extensively monitored, retrieving the extent of the unstable urban area and the velocity gradients toward the retaining structure, the discrete nature of MT-InSAR data and the medium resolution of S1 sensors presented a significant methodological challenge: the need to transition from a point-based characterization to a continuous representation of the deformation field.

While the use of geomatic data, particularly satellite data, remains indispensable due to its extensive coverage and historical depth, the true added value of this research lies in having critically addressed the intrinsic nature of the data. The study fully exploited the informational potential of the signal through advanced spatial analysis. The validation process followed a rigorous protocol: starting from data exploration and the definition of parameters for the application of the most appropriate Kriging method, the model developed on S1 data was initially subjected to internal validation, testing its consistency on portions of the original dataset. To strengthen the significance of the analysis and lay the groundwork for future developments, these results could be compared with data from the COSMO-SkyMed constellation; such external validation would further evaluate the solidity of the identified trends.

The originality of this work lies in the transformation of purely numerical and fragmented measurements into descriptive indicators of slope dynamics and, consequently, into predictive capabilities. The map produced is not a static snapshot, but an interpretive synthesis that allows for the hypothesis of future evolutionary trends of the phenomenon. The transition from the measured point to the continuous field enables the identification of acceleration trends and areas of potential instability propagation, providing a solid scientific basis for early warning models and the planning of targeted structural interventions.

Ultimately, this study demonstrates how the integration of geostatistical techniques can overcome the technological constraints of current sensors, serving as an effective decision-support tool.

References

1. Di Liddo, F., Locurcio, M., Morano, P., Fariello, F.: Towards a standardized framework: analyzing and systematizing urban sustainability indicators to guide effective city development. Land (Basel) **14** (2025). https://doi.org/10.3390/land14122369
2. Analisi del dissesto da frana in Puglia
3. Morano, P., Tajani, F., Locurcio, M.: Land use, economic welfare and property values: an analysis of the interdependencies of the real-estate market with zonal and socio-economic variables in the municipalities of apulia region (Italy). In: Sustainable Infrastructure: Breakthroughs in Research and Practice (2019). https://doi.org/10.4018/978-1-7998-0948-7.ch018
4. Solari, L., et al.: Review of satellite interferometry for landslide detection in Italy (2020). https://doi.org/10.3390/RS12081351
5. Mascitelli, A., et al.: Cultural heritage resilience in the face of extreme weather: lessons from the UNESCO site of alberobello. Sustainability (Switzerland) **15** (2023). https://doi.org/10.3390/su152115556
6. Parete, G., et al.: Climate impacts and adaptation strategies for coastal erosion, aquaculture, and tourism along the Adriatic side of Apulia region. Front. Clim. **6** (2024). https://doi.org/10.3389/fclim.2024.1378253
7. Tenuta, M., Dominici, R., Donato, P., Imbrogno, G., Lirer, S., De Rosa, R.: Approaches for the sustainable management of the Apulian coastal areas: the potential of a geoportal. Rendiconti Online della Società Geologica Italiana. **60**, 37–50 (2023). https://doi.org/10.3301/ROL.2023.29
8. Tajani, F., Bologna, A., Cerullo, G., Doko, E., Sica, F.: Upcycling strategies for resilience reconstruction goals: a case study of an italian public building. Buildings **15**, 3683 (2025). https://doi.org/10.3390/buildings15203683

9. Casagli, N., Intrieri, E., Tofani, V., Gigli, G., Raspini, F.: Landslide detection, monitoring and prediction with remote-sensing techniques. Nat. Rev. Earth Environ. **4**, 51–64 (2023). https://doi.org/10.1038/s43017-022-00373-x
10. Bianchini, S., Solari, L., Bertolo, D., Thuegaz, P., Catani, F.: Integration of satellite interferometric data in civil protection strategies for landslide studies at a regional scale. Remote Sens. (Basel) **13** (2021). https://doi.org/10.3390/rs13101881
11. Pagano, N., Sonnessa, A., Cotecchia, F., Tarantino, E.: Integrated use of geomatic methodologies for monitoring an instability phenomenon. In: Lecture Notes in Computer Science (including subseries Lecture Notes in Artificial Intelligence and Lecture Notes in Bioinformatics) (2023). https://doi.org/10.1007/978-3-031-37114-1_15
12. Sonnessa, A., di Lernia, A., Oscar Nitti, D., Nutricato, R., Tarantino, E., Cotecchia, F.: Integration of multi-sensor MTInSAR and ground-based geomatic data for the analysis of non-linear displacements affecting the urban area of Chieuti, Italy. Int. J. Appl. Earth Observat. Geoinf. **117** (2023). https://doi.org/10.1016/j.jag.2023.103194
13. Ma, P., et al.: Toward Fine Surveillance: a review of multitemporal interferometric synthetic aperture radar for infrastructure health monitoring. IEEE Geosci. Remote Sens. Mag. **10**, 207–230 (2022). https://doi.org/10.1109/MGRS.2021.3098182
14. Zhou, Y., Stein, A., Molenaar, M.: Integrating interferometric SAR data with levelling measurements of land subsidence using geostatistics. Int. J. Remote Sens. **24**, 3547–3563 (2003). https://doi.org/10.1080/0143116021000023880
15. Gagliardi, V., et al.: Testing sentinel-1 sar interferometry data for airport runway monitoring: a geostatistical analysis. Sensors **21** (2021). https://doi.org/10.3390/s21175769
16. Chen, L., Fang, Z., Xing, J., Cai, X.: How can geostatistics help us understand deep learning? An exploratory study in SAR-based aircraft detection. Int. J. Appl. Earth Observat. Geoinf. **134**, 104185 (2024). https://doi.org/10.1016/j.jag.2024.104185
17. Rutter, C.M., Isaaks, E.H., Srivastava, R.M.: An introduction to applied geostatistics. J. Am. Stat. Assoc. **86** (1991). https://doi.org/10.2307/2290613
18. Gioia, A., Bruno, M.F., Totaro, V., Iacobellis, V.: Parametric assessment of trend test power in a changing environment. Sustainability (Switzerland) **12** (2020). https://doi.org/10.3390/su12093889
19. Torres, R., et al.: GMES Sentinel-1 mission. Remote Sens. Environ. **120**, 9–24 (2012). https://doi.org/10.1016/j.rse.2011.05.028
20. Gulati, S., Nutricato, R., Nitti, D.O., Samarelli, S.: Spaceborne SAR interferometry exploitation for longitudinal ground deformation monitoring. In: 2021 IEEE Aerospace Conference (50100), pp. 1–10. IEEE (2021). https://doi.org/10.1109/AERO50100.2021.9438536
21. Okabe, A., Boots, B., Sugihara, K., Chiu, S.N., Kendall, D.G.: Spatial Tessellations: Concepts and Applications of Voronoi Diagrams (2025). https://doi.org/10.1002/9780470317013